

EFFECT OF MULLITE LAYER THICKNESS AND COMPOSITION ON FRACTURE TOUGHNESS OF LAYERED ALUMINA/MULLITE COMPOSITES

Henryk Tomaszewski¹⁾, Marek Boniecki¹⁾ and Helena Węglarz¹⁾

Laminar composites, containing layers of Al_2O_3 and either mullite or a mixture of mullite and Al_2O_3 were fabricated using a sequential centrifuging technique of water solutions containing suspended particles. Controlled crack growth experiments with notched beams of composites were done and showed the significant effect of barrier layer thickness and composition on crack propagation path during fracture. Distinct crack deflection in mullite layers was observed. Also, an increase of the crack deflection angle with the mullite layer thickness was found. In the case of barrier layers made of a mixture, crack deflection was not found independent of layer thickness. The observed changes were correlated with the distribution of residual stresses in layers created during cooling of sintered composites from their fabrication temperature. These residual stresses are a result of thermal expansion and sintering shrinkage mismatch of alumina and mullite.

1. INTRODUCTION

Ceramic materials are naturally brittle, so much effort has been directed to improve their toughness by various methods. Since the discovery of transformation toughening in ZrO_2 in 1975 [1] a variety of toughened ZrO_2 -based materials have been developed. The models presented [2-4] predict that the increase in toughness is linked with the size and shape of the transformation zone. A new way of optimising the transformation zone was developed by D.B. Marshall et al [5-6] in multilayered ceramic composites. A significant toughness increase of a Ce-TZP matrix with Al_2O_3 or $\text{Al}_2\text{O}_3/\text{ZrO}_2$ barrier layers was attributed to spreading of the transformation zone. In contrast with Marshall's results, H. Tomaszewski et al [7-8] showed that the main mechanism responsible for the toughness increase in ZrO_2 -based laminated composites is a crack deflection in

¹⁾ Instytut Technologii Materiałów Elektronicznych, 01-919 Warszawa, ul. Wólczyńska 133, e-mail: tomasz_h@sp.itme.edu.pl

the barrier layers caused by the presence of residual stress. The extent of the toughness increase was dependent on both layer thickness and composition. A correlation between crack deflection and distribution of compressive stresses in barrier layers of composites was also found.

In order to confirm these observations, alumina/mullite layered composites were prepared in present work and studied. In this case in the mullite layer with lower thermal expansion coefficient, α , ($\alpha_{\text{mullite}}=5 \times 10^{-6} \text{ } ^\circ\text{C}^{-1}$) a biaxial compressive stress was expected and similarly, a biaxial tensile stress in the alumina layer with higher α ($\alpha_{\text{Al}_2\text{O}_3}=9 \times 10^{-6} \text{ } ^\circ\text{C}^{-1}$). In such a stress distribution (Fig.1) the tensile stress in the alumina layer is expected to cause opening the crack in the notched beam during bending. On the contrary, the compressive stress in the mullite layer will prevent the opening of the crack.

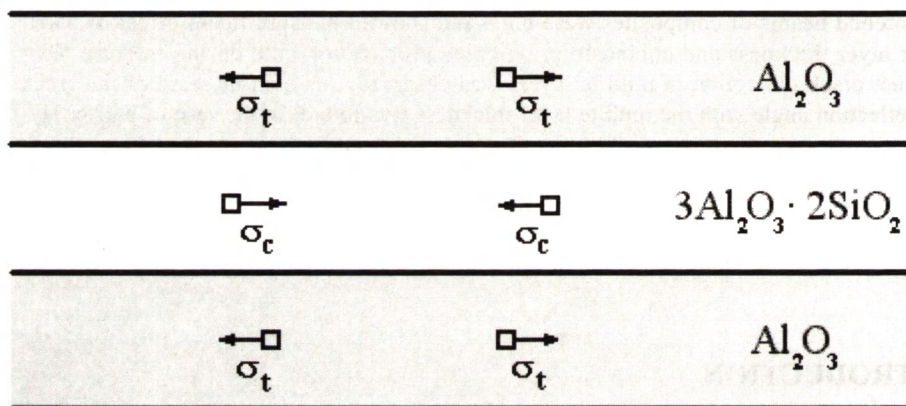


Fig.1. Expected stress distribution in layered alumina/mullite composites: σ_t - tensile stresses, σ_c - compressive stresses.

Rys. 1. Spodziewany rozkład naprężeń w kompozycie warstwowym tlenek glinu/mulit: σ_t - naprężenia rozciągające, σ_c - naprężenia ściskające.

2. EXPERIMENTAL PROCEDURE

Composites of Al_2O_3 /mullite with 25-75 μm thick layers were fabricated by sequential centrifuging (Model Z382, Hermle) of powder suspensions (Table I). Aqueous slurries containing 5 to 10wt% of powder were prepared by ultrasonically dispersing the powders in deionized water at pH 4. Cast samples were dried, additionally isostatically pressed at 120 MPa and then sintered at 1700 $^\circ\text{C}$. To minimize the shrinkage mismatch of Al_2O_3 and mullite, in some layered com-

posites a mixed composition of 50 vol% alumina and mullite was used instead of pure mullite. After sintering the samples were cut and ground to the dimensions of $45 \times 5 \times 5 \text{ mm}^3$ or $45 \times 6 \times 1.5 \text{ mm}^3$ and one surface perpendicular to the layers was polished. The sharp notch in the centre of the beams was prepared with two diamond saws: 0.200 and 0.025 mm thick.

Table 1. Ceramic powders used for preparing layered composites.

Tabela 1. Proszki ceramiczne stosowane do przygotowania kompozytów warstwowych.

Powder type	Producer	Grain size, μm	Sintering shrinkage, %	Application
Alumina	CEMAT, Poland	0.5	22.3	Matrix layer
Mullite SASM	Baikowski Chimie, France	0.7	18.4	Barrier layer

The bending strength of the composites was determined on square bars with dimensions $45 \times 5 \times 5 \text{ mm}^3$ perpendicular to the layers in three-point bending tests using a universal testing machine (Model 1446, Zwick) with 1mm/min loading speed and 40 mm bearing distance.

For measurement of Young's modulus the beams were trimmed to the height of 1 mm and then the compliance of the samples was recorded during loading tests with 0.1 mm/min loading speed and 40 mm bearing distance. The values of Young's modulus were determined using the relationship given by Fett and Munz [9], which is stated in equation (3) below.

The critical stress intensity factor, K_{Ic} , was measured following Evans [10] on notched beams ($45 \times 6 \times 1.5 \text{ mm}^3$, notch $\sim 1 \text{ mm}$) perpendicularly to the layers in a three-point bending test. The bearing spacing was 40 mm and rate of loading 1 mm/min.

The controlled crack growth tests were performed during three-point bending with 1 $\mu\text{m}/\text{min}$ loading speed and 40 mm bearing distance using the same testing machine. The crack was initiated and slowly grown by repeated loading and unloading. The procedure results in increase of crack length by one step less than 100 μm . The crack length, c , was measured *in situ* using a special device consisting of horizontal light microscope coupled with a CCD camera which were fitted to the testing machine by a system of elevator stages driven by stepping motors. This enabled the precise movement of the microscope objective in x-y-z directions for adjustment, focussing and tracking on the beam

side and bottom surface where the crack propagated. A measuring and registration system (framegrabber) was coupled to the load and strain system of the testing machine, and computer controlled both systems. The optical and electronic magnifications were about 250 x. The stress intensity factor, K_I , was calculated from the crack length, c , and force, P . The data of $K_I = f(c)$ obtained in the range of crack length studied were fitted by a linear function of $y = ax + b$ and the slope, a , was used as a parameter describing R-curve behaviour. All experiments were done at room temperature in normal air environments.

In several samples the crack growth tests were done without unloading. The time dependent displacement, d , of the sample was measured and recorded together with values of force, P . According to Fett and Munz [9], the total compliance, C , (which is given by equation (1))

$$C = \frac{d}{P} \quad (1)$$

consists of the compliance of the measuring system, C_u , the compliance of the uncracked bar, C_0 , and the portion ΔC caused by the crack.

$$C = C_u + C_0 + \Delta C \quad (2)$$

with
$$C_0 = \frac{L^2}{w^2 BE} \left[\frac{L}{4w} + (1+\nu) \frac{w}{2L} \right] \quad (3)$$

where E is Young's modulus, ν is Poisson's ratio, w is the specimen thickness, B is the specimen width and L is the bearing distance. The compliance part due to the crack was calculated using [9] as

$$\Delta C = 4.5 \frac{L^2}{w^2 EB} \left(\frac{a}{l-a} \right)^2 \sum_{i=0}^5 \sum_{j=0}^3 B_{ij} a^i \left(\frac{w}{L} \right)^j \quad (4)$$

with $a = \frac{c}{w}$, where c is the length of the crack and B_{ij} are the coefficients given by Fett and Munz [9].

The stress intensity factor K_I values have been determined from the relation (5)

$$K_I = 1.5 \frac{PL}{w^2 B} Y c^{\frac{1}{2}} \quad (5)$$

using the geometric function Y , stated below in equation (6), with the coefficients A_{ij} given by Fett and Munz [9].

$$Y = \frac{\sqrt{\Pi}}{(1-a)^{\frac{3}{2}}} \left[0.3738a + (1-a) \sum_{i,j=0}^4 A_{ij} a^i \left(\frac{w}{L} \right)^j \right] \quad (6)$$

By this procedure the maximal stress intensity factor, $K_{I_{max}}$, and the resistance to crack initiation, K_{I_r} were calculated. The crack growth rate $v=dc/dt$ controlled by the stress intensity factor, K_I , was calculated from the time dependent crack length, c . Assuming a power-law relation between v and K_I (equation 7), the parameters A (or $\log A$) and n were obtained.

$$v = \frac{dc}{dt} = AK_I^n \quad (7)$$

Given that the area under the recorded load-deflection curve of the specimen is the sum of the work used for the creation of two new surfaces and the elastic strain energy of the system and sample studied, the work-of-fracture, γ_F , was determined:

$$\gamma_F = U/2A \quad (8)$$

where U is the total deformation work of a specimen up to fracture and A is the area of fractured cross-section of the specimen.

Microstructure observations of composites studied were performed on polished surfaces by SEM using OPTON DSM950 microscope.

3. RESULTS

Controlled crack growth experiments indicated significant crack deflection in barrier layers of composites dependent on barrier thickness and composition, similarly to the results obtained for zirconia/alumina composites [7-8]. It oc-

curred that crack is deflected only in mullite layers (Fig.2) being under compressive stress. In alumina layers the crack deflects back to its original direction perpendicular to the layers. The degree of crack deflection is dependent on the mullite layer thickness. As can be seen from Table 2, the crack deflection angle increases with layer thickness. For example, in a 75 μm thick mullite layer the crack deflects over 90° . In layers with a thickness of 25 μm and lower, deflection does not take place.

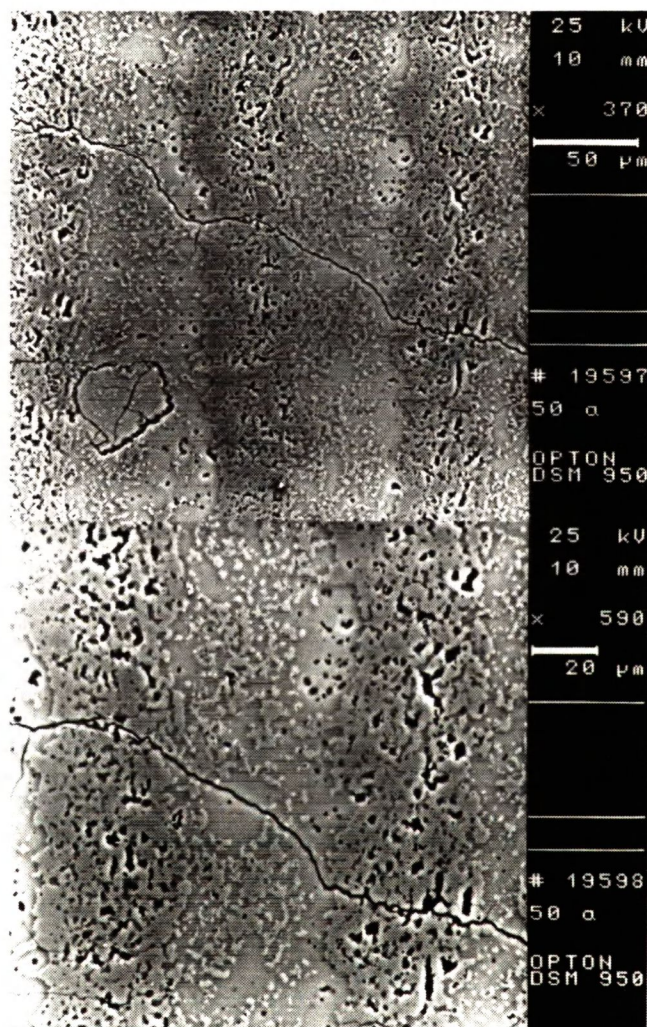


Fig. 2. Crack path in Al_2O_3 /mullite composite with 50 μm thick mullite barrier layers: the crack is deflected in mullite layers, in alumina layers it propagates perpendicularly to the layers.

Rys. 2. Droga pęknięcia w kompozycie tlenek glinu/mullit z warstwami mullitowymi o grubości 50 μm : pęknięcie odchyła się w warstwach mullitowych, w warstwach tlenku glinu natomiast propaguje prostopadle do kierunku ułożenia warstw.

Table 2. Crack deflection angle measured in the mullite layer of an alumina/mullite composite as a function of layer thickness.

Tabela 2. Kąty odchylenia pęknięcia mierzone w warstwie mulitowej kompozytu warstwowego w funkcji grubości warstwy.

Thickness of mullite layer, μm	25	50	75
Crack deflection angle, $^{\circ}$	0	48 ± 5	90

The character of the crack path changed strongly in composites with barrier layers made of a mullite and alumina mixture instead of pure mullite. Figs 3 and 4 show that the crack propagates through the barrier layers without deflection, for all the layer thicknesses studied.

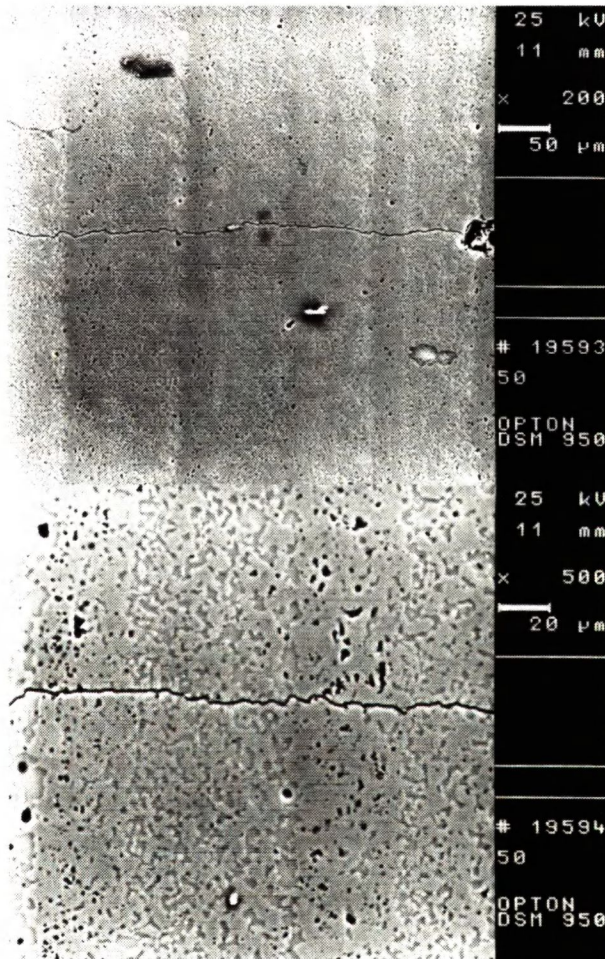


Fig. 3. Crack path in Al_2O_3 /mullite composite with 50 μm thick barrier layers made of a mullite and alumina mixture.

Rys. 3. Droga pęknięcia w kompozycie tlenek glinu/mulit z warstwami o grubości 50 μm zbudowanymi z mieszaniny mulitu i tlenku glinu.

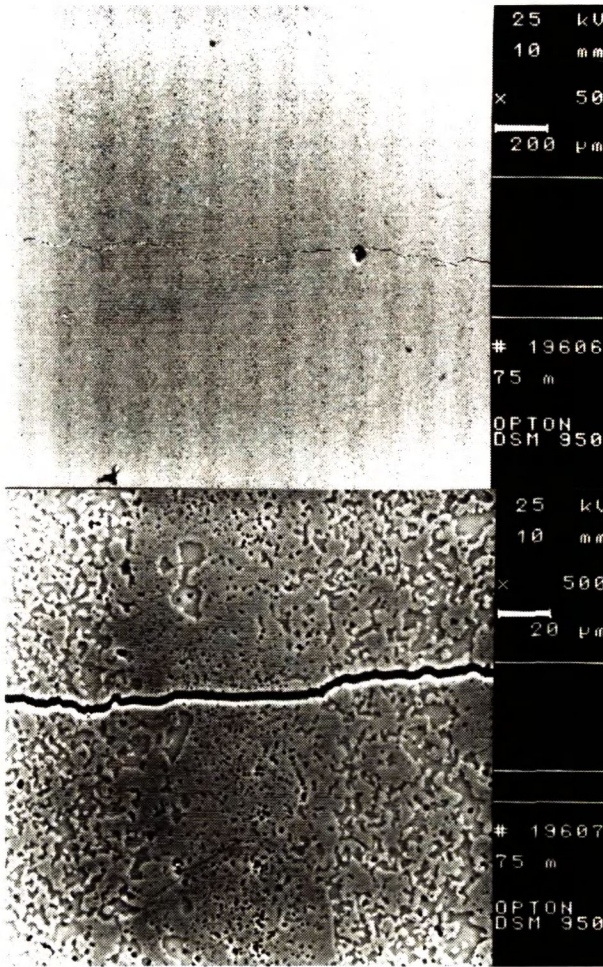


Fig.4. Crack path in Al_2O_3 /mullite composite with $75 \mu\text{m}$ thick barrier layers made of a mullite and alumina mixture.

Rys. 4. Droga pęknięcia w kompozycie tlenek glinu/mulitu z warstwami o grubości $75 \mu\text{m}$ zbudowanymi z mieszaniny mulitu i tlenku glinu.

Crack deflection in mullite layers dependent on layer thickness results in an increase in the slope parameter, a , describing the R-curve behaviour of composite studied. As can be seen from Table 3, the value of a equals 1.20 and 1.829 for composites with $50 \mu\text{m}$ and $75 \mu\text{m}$ thick mullite layers, respectively. For composites with a mixed barrier layer the corresponding parameter values are 0.402 and 0.641. It shows that deflection can be regarded as a more effective mechanism in increasing the fracture toughness as the crack growth (see Fig.5) than the bridging mechanism present in a pure alumina. For comparison, the parameter a for a pure alumina matrix studied is 0.606 (see Fig.6 and Table 4), which means that the toughness increases strongly namely from 3.6 to about $5.5 \text{ MPam}^{1/2}$ as the crack length increases up to 4.2 mm. However the increase in toughness becomes less pronounced when mullite is added. For a

mixed composition of 50 vol% alumina and mullite, the slope parameter decreases to 0.118. Decrease in parameter a means that mullite changes the residual stress state in the alumina matrix. The large thermal expansion mismatch between mullite and Al_2O_3 is thought to create additional regions of tension, as was found in Al_2O_3 -SiC system [11]. This in turn reduces the effectiveness of grain bridging and in consequence, the value of slope parameter a .

Table 3. Linear coefficients a and b (equation $y=ax+b$) for layered composites of alumina and mullite.

Tabela 3. Liniowe współczynniki a i b (równanie $y=ax+b$) dla kompozytów warstwowych tlenek glinu/mulit.

Type of barrier layers	Mullite		Mixture of mullite and alumina	
Layer thickness, μm	50	75	50	75
a	1.020 ± 0.193	1.829 ± 0.351	0.402 ± 0.108	0.641 ± 0.148
b	1.790 ± 0.367	1.613 ± 0.608	3.573 ± 0.410	3.152 ± 0.509

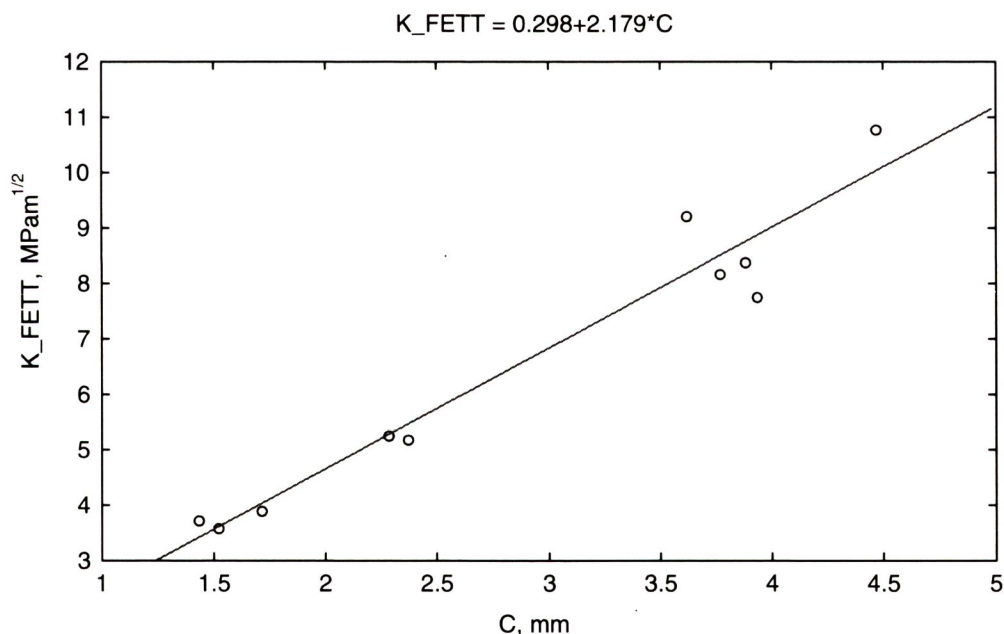


Fig. 5. Dependence of K_I on the crack length for a layered composite of alumina and mullite with 75 μm thick mullite layers.

Rys. 5. Zależność K_I od długości pęknięcia dla kompozytu warstwowego złożonego z warstw tlenku glinu i mulitu o grubości 75 μm .

Table 4. Linear coefficients a and b (equation $y=ax+b$) for alumina, mullite and a mixture of mullite and alumina.

Tabela 4. Liniowe współczynniki a i b (równanie $y=ax+b$) dla ceramiki z tlenku glinu, mulitu i mieszaniny mulit i tlenku glinu.

Type of ceramics	a	b
Alumina	0.606 ± 0.021	3.05 ± 0.03
Mullite	-0.058 ± 0.006	1.78 ± 0.01
Mixture of mullite and alumina	0.118 ± 0.049	2.82 ± 0.09

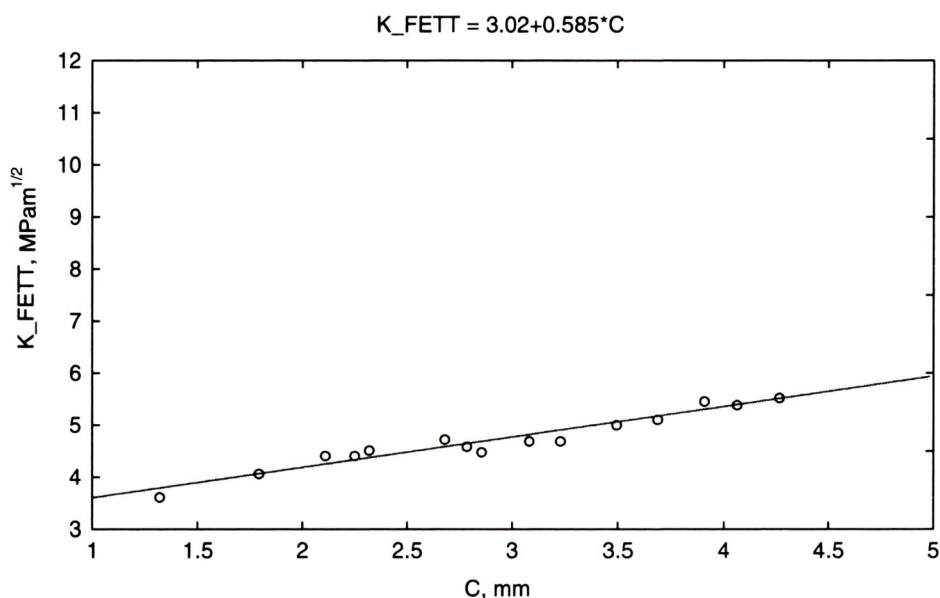


Fig. 6. Dependence of K_I on the crack length for an alumina matrix as used in layered composite preparation.

Rys. 6. Zależność K_I od długości pęknięcia dla ceramiki z tlenku glinu stosowanej do przygotowania kompozytów warstwowych.

Crack deflection in mullite layers results also in an increase in toughness of composites. Table 5 shows that the critical stress intensity factor, K_{Ic} , work-of-fracture, γ_F , and bending strength, σ_b , increase with the mullite barrier layer thickness and reach a maximum for the thickest layers. In the case of the thinnest layers, where crack deflection is not observed the above mentioned properties do not differ from the values obtained for composites with mixed barrier layers. Similar changes

are observed in the maximal stress intensity factor $K_{I_{max}}$, resistance to crack initiation K_{I_i} and crack growth rate parameter n .

Table 5. Mechanical properties of layered composites of alumina and mullite as a function of barrier layer thickness and composition.

Tabela 5. Własności mechaniczne kompozytów warstwowych tlenek glinu/mulit w funkcji grubości i składu warstw.

Type of barrier layer	Mullite			Mixture of mullite and alumina	
Layer thickness, μm	25	50	75	50	75
$\gamma_F, \text{J/m}^2$	26.65±2.39	57.54±1.09	76.24±1.25	39.39±5.89	40.43±4.57
$K_{Ic}, \text{MPam}^{1/2}$	4.14±0.52	4.55±0.22	5.85±0.19	3.87±0.31	4.27±0.53
σ_b, MPa	228.9±49.0	287.1±19.0	361.5±7.8	221.2±21.4	201.7±15.7
$K_{I_{max}}, \text{MPam}^{1/2}$	4.609±0.302	4.938±0.167	5.444±0.096	5.085±0.330	5.091±0.055
$K_{I_i}, \text{MPam}^{1/2}$	2.72±0.18	3.48±0.43	3.72±0.42	2.67±0.19	2.89±0.30
n	18.81±3.22	16.21±5.80	7.09±1.27	27.76±2.23	31.78±2.52
$\log A$	-15.81±3.22	-14.88±3.88	-8.83±0.06	-20.57±2.39	-25.96±2.36

The decreasing values of parameter n show that an initiated crack will propagate with lower rate in the case of composites with thicker mullite layers than in composites with the thinner layers. For comparison, the same properties of alumina, mullite and a homogenised mixture of mullite and alumina are presented in Table 6. Critical stress intensity factor, K_{Ic} , of mullite, resistance to crack initiation and bending strength are substantially lower than for alumina. On the other hand fracture toughness of a composite prepared from a homogenised mixture of mullite and alumina is not distinctly different from alumina ceramics. This can be a result of residual stresses present in this composite, where alumina grains are in tension but mullite grains in compression. Local compressive stress fields created by mullite grains can be responsible for the observed moderate decrease of composite bending strength in comparison to the pure alumina matrix.

However the large difference in fracture toughness properties between layered and homogenised composites, having the same volume composition of

mullite and alumina (see in Tables 5 and 6) seems to be a confirmation of the effect of deflection and the role of residual stress distribution in polycrystalline ceramic materials.

Table 6. Mechanical properties of alumina, mullite and a mixture of mullite and alumina.

Tabela 6. Mechaniczne własności ceramiki z tlenku glinu, mulitu i mieszaniny mulitu i tlenku glinu.

Type of ceramics	Alumina	Mullite	Mixture of mullite and alumina
K_{Ic} , MPam ^{1/2}	3.93±0.06	2.41±0.08	3.62±0.04
σ_b , MPa	328.5±25.5	153.5±12.5	277.5±26.4
$K_{I_{max}}$, MPam ^{1/2}	5.06±0.04	2.27±0.07	3.64±0.25
K_{Ii} , MPam ^{1/2}	2.96±0.09	1.75±0.17	2.76±0.04

4. DISCUSSION

Observations made by Ho et al [12] and Oechner et al [13] show that the stress state near the surface of the laminar composite specimen as presented in Fig.1 is more complex. These authors found edge cracks on the surface of the thin layers that were under nominal, residual compressive stress due to the biaxial constraint of an adjacent, thicker layer with a larger α . These edge cracks appeared near the centre of the layer, propagating into the layer and running parallel to the centreline. They showed that although biaxial compressive stresses exist in the layer far from the free surface, the stress distribution near the free surface is triaxial. Specifically, the component of the triaxial stress perpendicular to the centreline of the layer is a highly localised tensile stress, which diminishes in magnitude from the surface to the interior. Ho et al [12] observed that the occurrence of edge cracks was dependent on the thickness of the embedded layer and the magnitude of the residual compressive stress in the embedded layer. They found also that for a given residual stress, crack extension without any external stress takes place only when the layer thickness is higher than a critical value.

In our study the thickness of matrix and barrier layer was equal (25 to 75 μm) and edge cracks parallel to the layer were not found. In our opinion, crack deflection in mullite barrier layers is a result of interaction of three types

of stress. The first one is a residual compressive stress acting in the plane parallel to the layers present due to thermal expansion mismatch. The second is a perpendicular tensile stress found by Ho et al [12] and Oechner et al [13]. Both of these stress types are present in a laminate after cooling from fabrication temperature. And the third one is an external tensile stress applied in bending of the notched beam. The additional factor responsible for crack deflection can then be the compressive stress distribution in barrier layers. As it was found in layered composites of ZrO_2 and Al_2O_3 [7,8], the maximum compressive stress was observed at the interface and minimum in the centre of the alumina barrier layer. The value of minimum stress occurred to be dependent on layer thickness. According to Ho et al [12] and Oechner et al [13] the maximum of perpendicular tensile stress exists in the centre of the barrier layer and is also dependent on layer thickness. It means that in the centre of barrier layers with critical thickness perpendicular tensile stress dominates. As a result, the crack deflects in the centre of the thick layer and propagates along the layer. When the compressive stress increases from the minimum in the centre to the maximal value at the interface, then the crack deflects back to the original direction. In the case of the thinnest barrier layer the compressive stress across the layer is almost constant (the stress difference is at a minimum) but when perpendicular tensile stress in the centre reaches a minimum value the crack propagates through the layer without deflection. For intermediate thickness deflection of the crack at an angle of less than 90° is a result of combined stresses.

5. SUMMARY

The aim of this work was to investigate layered ceramic composites made of alumina matrix layers and mullite or mullite/alumina barrier layers. As it occurred, the distinct enhancement of toughness was found only for composite with mullite barrier layers. The controlled crack growth tests showed that the only mechanism responsible for the observed toughness increase was crack deflection. The degree of deflection was proportional to the mullite layer thickness. In the case of layer thickness lower than $25 \mu m$ the crack was not deflected during fracture. Crack deflection was not observed in the layers made of a mixture independently of layer thickness. Explanation of this phenomenon was given by analysis of stresses present in composite studied. The results obtained strongly confirm observations found for layered composites of alumina and

zirconia, namely that crack deflection in the barrier layers is a result of residual stresses generated by thermal expansion mismatch.

REFERENCES

- [1] Garvie R.C., Hannink R.H.J., Pascoe R.T., Nature, 248, 1975, 703
- [2] Evans A.G., Cannon R.M., Acta Metall., 34, 5, 1986, 651
- [3] McMeeking R.M, Evans A.G., J. Amer. Ceram. Soc., 65, 5, 1982, 242
- [4] Lambropoulos J.C., J. Amer. Ceram. Soc., 69, 3, 1986, 218
- [5] Marschall D.B., Lange F.F., Ratto J.J., J. Amer. Ceram. Soc., 74, 12, 1991, 2979
- [6] Marschall D.B, Ceram. Bull., 71, 6, 1992, 969
- [7] Tomaszewski H., Strzeszewski J., Gębicki W., J. Europ. Ceram. Soc., 19, 1999, 67
- [8] Tomaszewski H., Węglarz H., Boniecki M., Rećko M., J. Mat. Sci. 35, 2000, 4176
- [9] Fett T., Munz D., J. Amer. Ceram. Soc., 75, 4, 1992, 958
- [10] Bradt R.C., Hasselman D.P.H., Lange F.F.: Fracture Mechanics of Ceramics, Plenum Press, 1974, 1
- [11] Tomaszewski H., Boniecki M. Węglarz H., J. Europ. Ceram. Soc., 20, 2000, 1215
- [12] Ho S., Hillman C., Lange F.F. Suo Z., J.Amer. Ceram.Soc., 78, 9, 1995, 1353
- [13] Oechner M., Hillman C., Lange F.F., J.Amer.Ceram.Soc., 79, 7, 1996, 1834

WPLYW GRUBOŚCI I SKŁADU WARSTW MULITOWYCH NA ODPORNOŚĆ NA PĘKANIE WARSTWOWYCH KOMPOZYTÓW TLENEK GLINU/MULIT

STRESZCZENIE

Warstwowe kompozyty, zbudowane z warstw Al_2O_3 i mulitu lub mieszaniny mulitu i Al_2O_3 , wytwarzano metodą centrifugowania wodnych zawiesin proszków. Eksperymenty kontrolowanego rozwoju pęknięć wykazały istotny wpływ grubości i składu warstw na charakter drogi pęknięcia. W warstwach mulitowych zaobserwowano istotne odchylenie pęknięcia. Stwierdzono również wyraźną zależność pomiędzy kątem odchylenia pęknięcia i grubością warstw mulitowych. W przypadku warstw barierowych zbudowanych z mieszaniny mulitu i tlenku glinu nie zaobserwowano odchylenia pęknięcia, bez

względu na grubość warstw. Powyższe zmiany powiązano z rozkładem naprężeń wewnętrznych w warstwach, powstających podczas studzenia kompozytów od temperatury spiekania do temperatury otoczenia i będących wynikiem różnicy we własnościach cieplnych tlenku glinu i mulitu. Kolejnym źródłem naprężeń jest różnica w skurczliwości spiekania obu materiałów.